Above the Impact Zone: Aerial Imaging with AI-Based Rapid Flood Inundation Assessment Using EXIF-Tagged Imagery and Drone-to-Satellite Comparison

Vee Jay S. Lee[1], Aira Mae L. Marcelo[1], Lorenz S. Trinidad[1], Kennedy V. Rodriguez[1], Reynaldo L. De Asis[1]
[1]*Department of Computer Engineering, FEU Pampanga, City of San Fernando, Pampanga, Philippines*
Corresponding Author: leevjsoliman@feupampanga.edu.ph

Abstract: **Flood assessment in local disaster response is often delayed by limited access to inundated areas and reliance on ground-based observation. This study developed and evaluated a UAV-based aerial imaging system integrated with AI-assisted analysis for rapid flood inundation assessment using EXIF-tagged imagery and drone-to-satellite comparison. The system captures aerial images using a quadcopter platform, embeds GPS-based EXIF metadata, processes images through an AI analysis module, and compares drone imagery with ESRI World Imagery for geospatial validation. Controlled flight tests were conducted at 20 m, 40 m, 60 m, 80 m, and 100 m above ground level, while AI models were evaluated based on flood detection, response time, flood level estimation, and drone-to-satellite alignment. Results showed 100% successful flight trials across all tested altitudes, usable aerial image quality at 1920×1080 resolution, and increased ground coverage at higher altitudes. AI-based flood and non-flood detection achieved 100% accuracy across tested models, while GPT 4.1 Nano produced the fastest response time and Llama-4 obtained the highest mean satellite alignment. Expert evaluation by barangay and MDRRMO personnel indicated that the system was acceptable for flood monitoring and decision support. The developed system demonstrates potential as a rapid aerial assessment tool for local disaster response.**

Keywords: **UAV, aerial imaging, flood assessment, artificial intelligence, EXIF metadata, satellite comparison, disaster response.**

1. Introduction

Flooding remains one of the most frequent and destructive natural hazards worldwide, causing significant damage to infrastructure, economic loss, and risks to human life [1]. In the Philippines, flood events are commonly associated with typhoons, heavy rainfall, river overflow, and poor drainage conditions, particularly in low-lying and urbanized areas. These conditions require rapid and accurate assessment to support evacuation planning, emergency response, and resource allocation during disaster events [2].

Local disaster response in the Philippines is primarily managed by local government units (LGUs), particularly at the barangay and municipal levels. Barangay officials typically serve as the first observers of flood conditions, while Municipal Disaster Risk Reduction and Management Offices (MDRRMOs) are responsible for validating reports and making decisions for response operations. Despite this structured workflow, the availability of timely and accurate flood information remains limited, especially in areas that are inaccessible due to floodwater [3].

Traditional flood assessment methods rely heavily on ground-based observation, which can be time-consuming, labor-intensive, and hazardous to personnel. In many cases, delays in data collection reduce the effectiveness of disaster response operations. The increasing frequency and intensity of flood events further highlight the need for more efficient assessment approaches that can provide rapid situational awareness [1].

Recent advancements in unmanned aerial vehicles (UAVs), remote sensing, geographic information systems, and artificial intelligence (AI) have enabled new approaches for environmental monitoring and disaster management. UAVs, in particular, offer the capability to capture high-resolution aerial images in real time and access hazardous or hard-to-reach locations. These capabilities make UAVs suitable for flood observation and mapping applications [4]. When combined with AI-based image analysis, UAV systems can automatically detect flood conditions, estimate water coverage, and generate meaningful insights from aerial imagery [5].

Furthermore, digital images captured by UAVs can include Exchangeable Image File Format (EXIF) metadata, which contains geospatial information such as GPS coordinates, timestamps, and camera parameters. This enables location-based analysis and supports satellite imagery for spatial validation. Satellite data, such as ESRI World Imagery, provides a broader geographic reference that can be used to compare and verify UAV-captured images [6].

Although previous studies have explored UAV-based flood monitoring and AI-assisted flood detection, many focus primarily on algorithm development or controlled experimental environments. There is limited research on integrated systems

that combine UAV aerial imaging, EXIF metadata processing, AI-based image interpretation, and drone-to-satellite comparison into a practical workflow for disaster response, particularly at the local government level [5].

To address this gap, this study proposes and evaluates a UAV-based aerial imaging system integrated with AI-assisted analysis for rapid flood inundation assessment. The system utilizes EXIF-tagged imagery, geospatial processing, and drone-to-satellite image comparison to generate structured flood assessment outputs. The study is implemented within the context of the barangay-to-MDRRMO reporting workflow in Pampanga, Philippines.

The main contribution of this research is the development of an integrated flood assessment system that combines UAV aerial imaging, geospatial metadata, artificial intelligence, and satellite comparison to support rapid and location-based flood analysis. The system is evaluated in terms of UAV flight performance, image quality, area coverage, video transmission reliability, AI-based flood detection, flood level estimation, drone-to-satellite alignment, and expert-based acceptability.

2. Methodology

A. Research Design

The study followed an evolutionary prototyping approach, where the prototype was progressively designed, tested, evaluated, and improved based on technical testing and expert feedback. The development process included UAV hardware integration, ground station development, camera and video transmission setup, EXIF-tagged image acquisition, AI-assisted image analysis, drone-to-satellite comparison, and expert-based system evaluation.

The evaluation was structured into two main components. The first component involved technical testing of the UAV platform, image acquisition system, AI analysis module, and drone-to-satellite comparison process. The second component involved expert evaluation by barangay officials and MDRRMO personnel using a structured questionnaire based on the ISO/IEC/IEEE 15288 system life cycle framework [7].

B. UAV Hardware Integration

The UAV platform was developed using a quadcopter configuration designed for aerial flood observation and image acquisition. The hardware integration included the power subsystem, flight controller, receiver, telemetry module, sensors, propulsion system, imaging subsystem, and video transmission components. These subsystems were integrated to support stable UAV operation, real-time communication, and aerial image capture during flood monitoring activities.

The UAV system used an F450 quadcopter frame, Pixhawk 2.4.8 flight controller, GPS modules, Racerstar BR2216 810 kV motors, EMAX BLHeli 40A electronic speed controllers, Flysky FS-i6X transmitter and IA10B receiver, MicoAir MTF-01P sensor, CaddxFPV Ratel Pro camera, Rush Tank Max Solo 5.8 GHz video transmitter, RC832 HD receiver, UGREEN HDMI capture card, ToolkitRC M6D charger, and 24V 25A 600W power supply. These components were selected to support UAV stability, image quality, video transmission, GPS-based operation, and reliable power management.

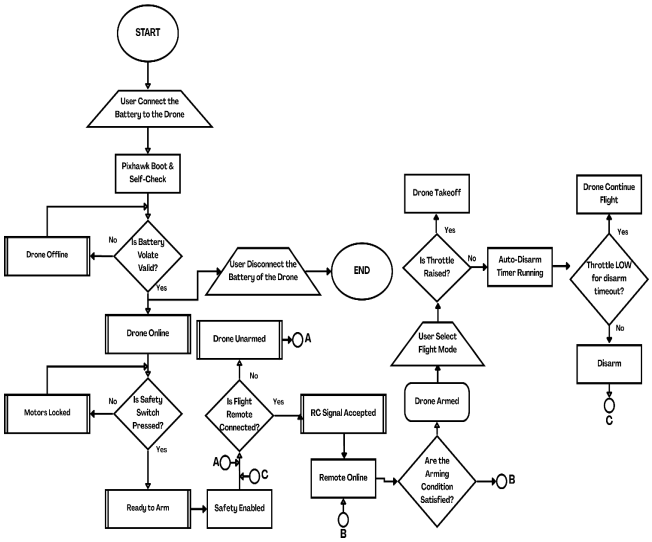

Fig. 1. Hardware Integration Workflow of the UAV-Based Flood Assessment System

The hardware integration workflow of the developed UAV system is shown in Figure 1. The figure presents the interconnection of the main UAV subsystems, including flight control, power distribution, telemetry, sensing, propulsion, and imaging components.

C. Ground Station and EXIF-Tagged Image Acquisition

The ground station served as the central interface for UAV flight monitoring, camera operation, image capture, and EXIF metadata integration. Mission Planner version 1.3.83 was used for flight planning, waypoint execution, and real-time telemetry monitoring. A Python-based camera dashboard was developed to receive the UAV video feed, capture aerial images, and associate the captured images with telemetry-based geospatial information.

During flight operations, the UAV captured aerial images using a gimbal-mounted camera primarily positioned in a 90° downward-facing orientation. This configuration was used to capture roads, structures, visible floodwater, and surrounding environmental features from an aerial perspective. The system embedded GPS coordinates, timestamps, and camera-related information into the captured images using EXIF metadata. This allowed each aerial image to be linked to a specific geographic location for flood assessment and satellite comparison.

The UAV was operated using Loiter mode and Auto mode for controlled image acquisition. Loiter mode supported stable hovering during image capture, while Auto mode enabled waypoint-based mission execution for consistent aerial coverage. Controlled flight tests were conducted at 20 m, 40 m,

60 m, 80 m, and 100 m above ground level to evaluate altitude stability, image perspective, and visible ground coverage.

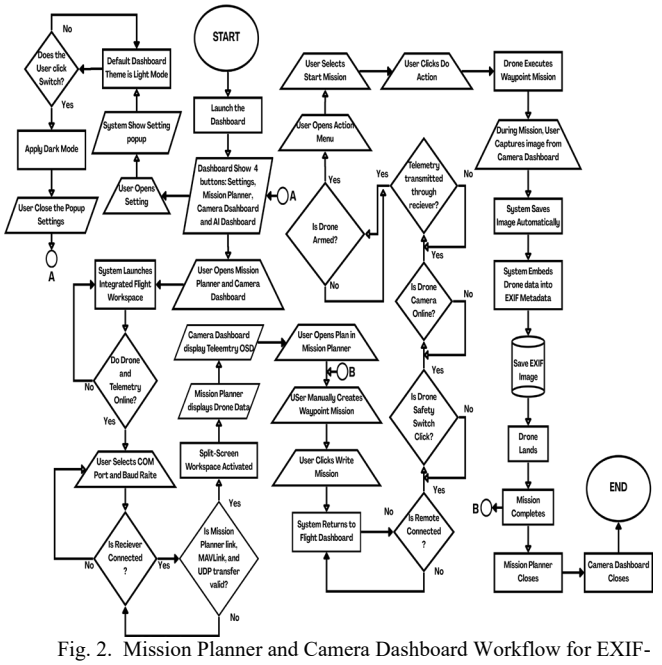

Fig. 2. Mission Planner and Camera Dashboard Workflow for EXIF-Tagged Image Acquisition

Figure 2 presents the ground station workflow used for mission planning, pre-flight checking, waypoint execution, real-time camera monitoring, image capture, and EXIF metadata integration.

D. AI-Assisted Flood Analysis and Drone-to-Satellite Comparison

The AI-assisted flood analysis module was implemented through a Python-based API system. Captured aerial images were converted into Base64-encoded image data and processed by the AI module together with geospatial information extracted from EXIF metadata. The AI model evaluated visible indicators of flooding, including surface water accumulation, road visibility, affected structures, and surrounding environmental conditions.

The system used EXIF-based GPS coordinates to identify the geographic location of each captured image. The same coordinates were used to retrieve corresponding satellite reference imagery from ESRI World Imagery. The drone image and satellite image were compared to support spatial validation and determine whether the UAV-captured scene corresponded to the correct geographic location.

Several AI models were evaluated in the study, including GPT 4.0, GPT 4.1, GPT 4.1 Mini, GPT 4.1 Nano, Phi-4, and Llama-4. The models were assessed based on their ability to process EXIF-tagged aerial images, detect flood and non-flood conditions, estimate flood level, generate structured flood assessment outputs, and support drone-to-satellite image alignment.

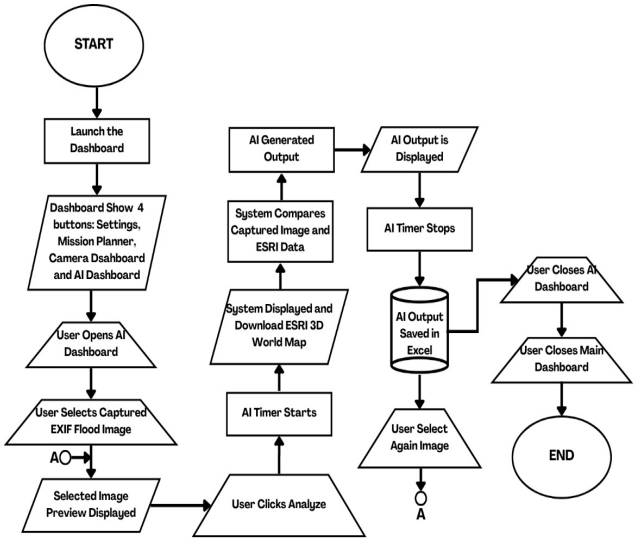

Fig. 3. AI Dashboard Workflow for flood Analysis and Drone-to-Satellite Comparison

The AI dashboard workflow for image selection, preview, AI-based flood analysis, satellite image comparison, output generation, and result storage is shown in Figure 3.

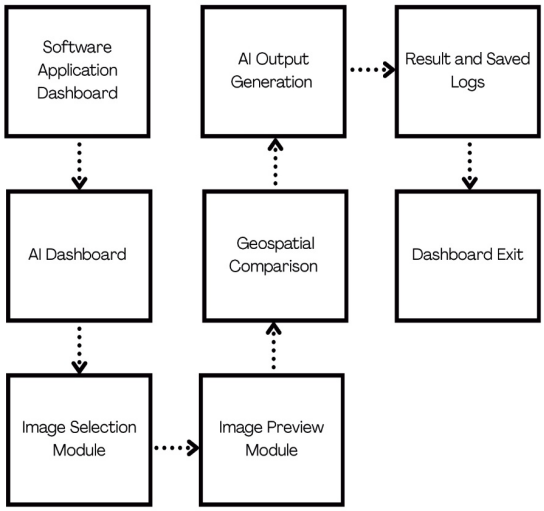

Fig. 4. Block Diagram of the AI-Based Geospatial Flood Assessment Workflow

Figure 4 further illustrates the technical processing pipeline of the AI-assisted geospatial flood assessment workflow, showing how aerial images, EXIF metadata, satellite imagery, and AI-generated outputs are integrated.

E. Flood Classification and Hazard Reference

Flood classification in this study was based on flood susceptibility criteria aligned with Republic Act No. 10121 and local disaster risk reduction references. The system used flood height, duration, and barangay-level hazard classification to support the interpretation of AI-generated flood assessment outputs. The classification categories included low, moderate, and high susceptibility levels.

Table 1
Criteria for Flood Zone Matrix (Adapted from RA 10121, Section 7)

Level of Susceptibility	Flood Height	Duration	Interpretation
Low	≤ 0.5 m	1	Areas are likely to experience flood heights of 0.5 m or less or flood duration of less than 1 day.
Moderate	0.5–1 m	1 – 3	Areas likely to experience flood heights between 0.5–1 m or flood duration of 1–3 days.
High	> 1 m	> 3	Areas likely to experience flood heights above 1 m or flood duration longer than 3 days. These areas are immediately flooded during heavy rains.

The flood susceptibility criteria used to classify flood hazard levels based on flood height and duration are presented in Table 1.

A barangay-level flood depth classification was also used to interpret flood height estimates in feet. This classification categorized flood depth into low, moderate, and high levels using practical water depth ranges. Low susceptibility corresponded to water depth of 2 ft or below, moderate susceptibility corresponded to 2.1–3.9 ft, and high susceptibility corresponded to water depth above 4.0 ft.

Table 2
Flood Depth-Based Hazard Classification for Philippine Barangay (Derived from RA 10121, DRRMOs, and Local Disaster Experience)

Level of Susceptibility	Water Depth (ft)	Color Code	Interpretation
Low	≤ 2	Yellow	Minor flooding: water level typically reaches streets and ground floors of houses; generally passable with minimal disruption.
Moderate	2.1–3.9	Orange	Moderate flooding: water may enter houses, covering floors and furniture; movement becomes more difficult; caution advised.
High	> 4.0	Red	High flooding: water reaches mid-level houses or higher; significant disruption to daily activities and movement; emergency response may be required.

The barangay-level flood depth classification used for interpreting AI-generated flood level estimates is shown in Table 2.

The system also integrated a Pampanga flood susceptibility dataset derived from the Flood Hazard Map of Pampanga prepared by the Pampanga Provincial Disaster Risk Reduction and Management Office. The dataset classified barangays in each municipality or city according to High, Mid-High, Low-High, Low-Mid, and Low susceptibility categories. This dataset served as a geographic hazard reference for validating and contextualizing the flood assessment output generated by the system.

Table 3 Pampanga Flood Susceptibility Dataset Used as Geographic Hazard Reference

Municipality / City	Total Barangays	High	Mid-High	Low-High	Low-Mid	Low
Apalit	12	1	2	6	2	1
Arayat	30	0	4	24	2	0
Bacolor	21	3	1	15	2	0
Candaba	33	3	19	11	0	0
City of San Fernando	35	1	5	14	6	9
Floridablanca	33	0	4	22	3	4
Guagua	31	1	14	15	1	0
Lubao	44	4	13	24	3	0
Mabalacat City	27	0	0	17	3	7
Macabebe	25	20	5	0	0	0
Magalang	27	0	3	17	7	0
Masantol	26	25	1	0	0	0
Mexico	43	0	11	25	5	2
Minalin	15	0	3	8	4	0
Porac	29	0	1	25	0	3
San Luis	17	3	6	6	2	0
San Simon	14	0	4	7	3	0
Santa Ana	14	0	0	13	1	0
Santa Rita	10	0	0	9	1	0
Sasmuan	12	5	0	7	0	0
Santo Tomas	7	0	2	5	0	0

The Pampanga flood susceptibility dataset used as the geographic hazard reference of the system is presented in Table 3.

F. System Testing Procedure

The system testing procedure was conducted to evaluate the operational performance of the UAV platform, image acquisition process, AI-assisted analysis, and drone-to-satellite comparison. The technical testing focused on flight altitude and stability, camera resolution and image quality, area coverage, video transmission consistency, EXIF image processing, flood detection performance, flood height estimation, and satellite image alignment.

Flight tests were performed at 20 m, 40 m, 60 m, 80 m, and 100 m above ground level. These altitude levels were used to determine how flight height affected image perspective, visible ground coverage, and UAV stability. The operational flood-image acquisition range was discussed within 50 m to 100 m above ground level, which provided broader area visibility while remaining below the 120 m AGL ceiling generally applied in Philippine drone operations.

Image quality testing evaluated whether the captured aerial images were sufficiently clear for flood observation and AI-assisted interpretation. The system emphasized 1920×1080 resolution because this setting produced lower noise and clearer image output compared with lower resolutions. Video transmission testing considered dropout events and blackout frames to determine the reliability of real-time visual monitoring from the UAV to the ground station.

AI testing evaluated the performance of each model in terms of flood/non-flood detection, response time, flood level

estimation, and drone-to-satellite alignment. The AI-generated outputs were compared with reference flood observations and measured flood depth data to determine accuracy and consistency. Drone-to-satellite comparison was evaluated by comparing UAV-captured images with satellite reference imagery retrieved using the same EXIF-based coordinates.

G. Respondents, Instrument, and Data Analysis

The expert evaluation involved 11 respondents selected through purposive sampling. The respondents consisted of 4 barangay officials and 7 MDRRMO personnel. Barangay officials represented the community-level flood observation and reporting layer, while MDRRMO personnel represented the municipal-level disaster validation and decision-support layer. These respondents were selected because of their roles and experience in flood monitoring, disaster reporting, and local disaster response activities.

A structured questionnaire was used to evaluate the developed system. The questionnaire was based on ISO/IEC/IEEE 15288 and focused on system design and architecture, verification and validation procedures, and hardware–software integration performance. The questionnaire used a four-point Likert-type scale, where 4 represented Strongly Agree, 3 represented Agree, 2 represented Disagree, and 1 represented Strongly Disagree.

The instrument underwent expert validation to establish face and content validity. The validation was conducted by engineering and research experts who reviewed the clarity, appropriateness, and alignment of the questionnaire items with the research objectives and system evaluation criteria.

Table 4
Verbal Interpretation and Acceptability Level of the Four-Point Likert-Type Scale

Scale	Range Value	Verbal Interpretation	Acceptability Level
4	3.51-4.00	Strongly Agree	Highly Acceptable
3	2.51-3.50	Agree	Acceptable
2	1.51-2.50	Disagree	Less Acceptable
1	1.00-1.50	Strongly Disagree	Not Acceptable

Note. SA = Strongly Agree; A = Agree; D = Disagree; SD = Strongly Disagree.

The verbal interpretation and acceptability level used for the four-point Likert-type evaluation scale are presented in Table 4.

The collected technical data were analyzed using descriptive statistics, including frequency count, success rate, minimum and maximum values, range, mean, standard deviation, and ratio-based measures. These statistical measures were used to summarize flight stability, image quality, video transmission behavior, area coverage, AI model performance, flood level estimation, and drone-to-satellite image alignment.

For expert evaluation, weighted mean was used to determine the acceptability of the developed system based on the responses from barangay officials and MDRRMO personnel. The computed mean scores were interpreted using the four-point Likert-type scale shown in Table 4. This allowed the study to determine the system's acceptability in terms of functionality, reliability, usability, effectiveness, and practical applicability in local flood assessment.

3. Results and Discussion

A. UAV Flight Stability and Altitude Accuracy

The UAV platform was evaluated at five hover altitudes: 20 m, 40 m, 60 m, 80 m, and 100 m above ground level. The results showed that the UAV successfully completed all test trials at each altitude, producing a 100% success rate across all tested flight levels. This indicates that the developed UAV platform was capable of maintaining stable operation within the tested altitude range for aerial flood observation.

Table 5
UAV Flight Stability and Altitude Accuracy at Different Hover Altitudes

Image quality metric	Image Quality Test Results							
	1920×1080		1280×720		853×480		640×360	
	Mean	SD	Mean	SD	Mean	SD	Mean	SD
Sharpness	69.97	5.80	174.94	16.90	579.41	51.43	1283.34	99.73
Noise	4.67	0.20	7.83	0.31	12.29	0.40	15.63	0.42
Contrast	44.62	1.41	44.58	1.41	44.55	1.41	44.47	1.41
Saturation	93.70	11.55	92.82	11.45	92.38	11.39	91.93	11.32
Color cast index	5.47	0.89	5.46	0.89	5.45	0.89	5.45	0.89

Note: n = number of successful trials; Min = minimum; Max = maximum; R = range; SD = standard deviation. Recorded wind speed ranged from 1.09 m/s to 5.83 m/s, corresponding to light to moderate wind conditions during the UAV flight tests.

The altitude readings remained close to the target values, with low altitude variability across the five test levels. The altitude standard deviation was not higher than 0.30 m, showing that the UAV maintained consistent altitude control during hover operations. Orientation stability also improved at higher altitudes, as roll, pitch, and yaw variability generally decreased from lower-altitude to higher-altitude tests. This suggests that the UAV experienced more stable hover behavior from 60 m to 100 m compared with the lower-altitude flights.

These findings confirm that the UAV platform was suitable for controlled aerial image acquisition. Stable altitude control is important in flood assessment because inconsistent flight height may affect image scale, ground coverage, and the accuracy of visual interpretation. The results therefore support the use of the UAV platform for systematic flood observation within the tested altitude range.

B. Image Quality Performance Across Camera Resolutions

Image quality was evaluated across different camera resolutions to determine the most suitable setting for AI-assisted flood interpretation. The results showed that the

1920×1080 resolution produced the most useful image quality for flood assessment. This setting obtained the lowest noise value of 4.67 and provided clearer image output for visual inspection and AI-based analysis.

Table 6
Image Quality Performance Across Different Camera Resolutions

Performance metric	Flight Altitude Test Results					
	Notation	20 m	40 m	60 m	80 m	100 m
Successful trials	n	25	25	25	25	25
Success rate	%	100	100	100	100	100
Minimum attained altitude	Min	19.65	39.76	59.69	79.62	99.46
Maximum attained altitude	Max	20.81	40.41	60.34	80.83	100.40
Observed altitude range	R	1.16	0.65	0.65	1.21	0.94
Altitude variability	SD	0.27	0.30	0.16	0.15	0.20
Roll variability	SD	1.62	1.48	0.72	1.13	1.01
Pitch variability	SD	4.11	1.18	0.77	1.14	1.06
Yaw variability	SD	5.77	6.33	2.09	2.84	1.75

Note: SD = standard deviation. Sharpness was based on the variance of the Laplacian, noise on the standard deviation of the high-pass residual, contrast on the grayscale standard deviation, saturation on the mean HSV saturation, and color cast index on the scaled deviation of the normalized RGB channel means from neutral gray.

Lower image resolutions showed increased noise and higher sharpness variability, which may reduce the consistency of image interpretation. Although lower-resolution images may still be usable for general viewing, the reduced image clarity can affect the visibility of flood indicators such as water-covered roads, submerged ground surfaces, and nearby structures.

The 1920×1080 resolution was therefore considered the most appropriate setting for the system because it provided clearer visual detail while supporting AI-assisted analysis. This result is important because the AI module depends on image clarity to identify visible flood conditions, estimate flood levels, and compare the captured UAV image with satellite reference imagery.

C. Video Transmission Reliability

Video transmission reliability was evaluated to determine whether the UAV could provide stable visual feed from the aerial platform to the ground station. The results showed that video transmission remained generally stable up to 100 m. However, signal quality decreased as the UAV altitude and distance increased. The signal-to-noise ratio decreased from 30.42 dB at 20 m to 28.58 dB at 100 m, while dropout and blackout events were observed mainly at 60 m and 100 m.

Table 7
Video Transmission Reliability at Different Flight Altitudes

Distance (m)	Video Metadata			
	Mean SNR (dB)	Mean Sharpness	Dropout Events	Blackout Frames
20	30.42	207.25	0	0
40	29.07	310.21	0	0
60	28.79	313.89	2	8
80	28.67	307.79	0	0
100	28.58	320.8	3	24

The increase in dropout and blackout frames at higher altitudes indicates that analog video transmission performance may be affected by flight distance, antenna orientation, environmental interference, and signal strength. Despite these limitations, the system remained usable for image acquisition and monitoring within the tested range.

These results suggest that the current video transmission setup is acceptable for controlled aerial flood observation, but improvements may be needed for longer-range or more demanding field operations. Upgrading to a digital transmission system or improving antenna configuration may further reduce signal interruptions and improve real-time monitoring reliability.

D. Video Transmission Reliability

Ground coverage was evaluated to determine how flight altitude affected the visible area captured by the UAV. The results showed that ground coverage increased as flight altitude increased. At 20 m, the estimated ground coverage was 673.15 m², while at 100 m, the coverage increased to 17,525.4 m². This indicates that higher flight altitudes allow the UAV to observe wider areas, which is useful for rapid flood assessment.

Table 8
Ground Coverage Area at Different UAV Flight Altitudes

Altitude (m)	Area Coverage		
	Manual Estimated Area (m²)	Image-Based Estimated Area Range (m²)	Theoretical Area Range (m²)
20	673.15	600 – 700	665 – 735
40	2,706.67	2,400 – 2,800	2,660 – 2,940
60	6,061.88	5,800 – 6,500	5,985 – 6,615
80	11,010.23	10,500 – 11,500	10,640 – 11,760
100	17,525.4	16,600 – 18,500	16,650 – 18,400

The comparison among manual estimates, image-based estimates, and theoretical estimates showed consistent results, confirming the reliability of the ground coverage measurement. Wider coverage at higher altitudes is useful for identifying the general extent of flooding, affected roads, and visible water accumulation. However, higher altitude may also reduce image

detail, which must be considered when selecting flight height for actual flood observation.

The findings show a trade-off between coverage and detail. Lower altitudes provide closer visual detail, while higher altitudes provide broader situational awareness. For operational flood-image acquisition, the 50 m to 100 m range is suitable because it provides broader visibility while still maintaining usable image quality for AI-assisted flood assessment.

E. AI odel Performance for Flood and Non-Flood Image Analysis

The AI-assisted flood analysis module was evaluated using multiple AI models, including GPT 4.0, GPT 4.1, GPT 4.1 Mini, GPT 4.1 Nano, Phi-4, and Llama-4. The models were tested for flood and non-flood image analysis, response time, and output generation. Results showed that all tested models achieved 100% accuracy in flood and non-flood detection.

Table 9
AI Model Performance for Flood and Non-Flood Image Analysis

Models	AI Output Analysis				
	Flood Detection (%)	Non-Flood Detection Success Rate (%)	Overall Accuracy (%)	Mean Response Time (s)	Max Requests/ Day
GPT 4.0	100	100	100	12.07	48
GPT 4.0 Mini	100	100	100	24.07	106
GPT 4.1	100	100	100	12.99	48
GPT 4.1 Mini	100	100	100	11.85	147
GPT 4.1 Nano	100	100	100	7.36	147
Phi-4-Multimodal-Instruct	100	100	100	9.7	35
Llama-4-Maverick-17B-128E-Instruct-FP8	100	100	100	8.9	50

Among the tested models, GPT 4.1 Nano produced the fastest mean response time of 7.36 s. This result indicates that GPT 4.1 Nano is suitable for rapid flood assessment tasks where shorter processing time is needed. GPT 4.1 Mini and GPT 4.1 Nano also showed the highest maximum daily request capacity, with 147 requests per day, making them practical options for repeated image analysis during field deployment.

The 100% flood/non-flood detection accuracy demonstrates that the AI-assisted module can correctly classify visible flood conditions from UAV-captured images under the tested conditions. However, response time, request limitations, alignment performance, and flood level estimation accuracy should also be considered when selecting the most appropriate AI model for operational use.

F. Drone-to-Satellite Image Alignment Performance

Drone-to-satellite image comparison was evaluated to determine how well the AI models aligned UAV-captured images with satellite reference imagery from ESRI World Imagery. The results showed that Llama-4-Maverick achieved the highest mean alignment score of 92.2%, followed by GPT 4.1 with 90%. Other models produced alignment scores ranging from 65% to 85%.

Table 10
Drone-to-Satellite Image Alignment Performance of AI Models

AI Models	Drone and Satellite Image Alignment			
	Total Trials	Min Alignment (%)	Max Alignment (%)	Mean Alignment (%)
GPT 4.0	25	85	85	85
GPT 4.0 Mini	25	85	85	85
GPT 4.1	25	90	90	90
GPT 4.1 Mini	25	85	85	85
GPT 4.1 Nano	25	65	65	65
Phi-4-Multimodal-Instruct	25	80	85	80.2
Llama-4-Maverick-17B-128E-Instruct-FP8	25	90	95	92.2

The high alignment scores of Llama-4-Maverick and GPT 4.1 suggest that these models were more effective in comparing UAV imagery with satellite reference data. This is important because the system uses drone-to-satellite comparison to support spatial validation and verify that the captured UAV image corresponds to the intended geographic location.

Although the best-performing model reached 92.2% mean alignment, no model exceeded 95% alignment. This suggests that future improvements may be needed in GPS accuracy, camera calibration, image matching, and satellite reference retrieval. Nevertheless, the results demonstrate that drone-to-satellite comparison can strengthen the reliability of UAV-based flood assessment by adding a geospatial validation layer to AI-generated outputs.

G. Flood Level Estimation Accuracy

Flood level estimation was evaluated by comparing AI-generated flood level outputs with measured flood depth references. The results showed that most AI models achieved 100% flood level estimation accuracy, while Phi-4-Multimodal-Instruct produced 0% accuracy. The accurate models classified flood levels into moderate or high categories depending on the measured reference values.

The results indicate that most tested AI models were capable of generating flood level estimates that matched the reference classification. This supports the potential use of AI-assisted interpretation for preliminary flood level assessment. However, the poor performance of Phi-4 shows that not all multimodal models are equally reliable for flood depth interpretation.

Table 11
Flood Level Estimation Accuracy of AI Models

AI Models	AI Output Analysis				
	Min Encoded Value	Max Encoded Value	Mean Encoded Value	Estimated Flood Level	Accuracy (%)
GPT 4.0	1	2	1.16	Moderate	100
GPT 4.0 Mini	2	2	2.00	High	100
GPT 4.1	2	2	2.00	High	100
GPT 4.1 Mini	2	2	2.00	High	100
GPT 4.1 Nano	1	1	1.00	Moderate	100
Phi-4-Multimodal-Instruct	0	0	0.00	Low	0
Llama-4-Maverick-17B-128E-Instruct-FP8	1	1	1.00	Moderate	100

These findings suggest that AI-based flood level estimation should be validated before deployment in actual disaster response settings. Although several models performed well in the study, AI-generated outputs should still be treated as decision-support information rather than a replacement for field validation or official disaster assessment.

H. Barangay and MDRRMO System Evaluation

The developed system was evaluated by barangay officials and MDRRMO personnel to determine its practical acceptability for flood monitoring and disaster response support. The barangay evaluation showed positive results across design clarity and applicability, system testing and reliability, and hardware–software performance. The overall means were 3.50 for design clarity and applicability, 3.70 for system testing and reliability, and 3.60 for hardware and software performance. These results correspond to "Agree" and "Strongly Agree" interpretations.

The MDRRMO evaluation also showed favorable results. Output clarity obtained an overall mean of 3.23, usefulness for decision-making obtained 3.49, and accuracy and reliability obtained 3.37. These scores were interpreted as "Agree," indicating that MDRRMO personnel found the system useful and acceptable for supporting flood assessment and decision-making activities.

The evaluation results show that both barangay officials and MDRRMO personnel recognized the system's potential for local flood monitoring. Barangay officials gave higher ratings, particularly in system reliability and hardware–software performance, suggesting that the system is useful at the community observation level. MDRRMO personnel also agreed that the system could support output clarity, decision-making, and reliability in disaster response planning.

Table 12
Summary of Barangay and MDRRMO System Evaluation Results

Evaluation Group	Evaluation Dimension	Mean	Verbal Interpretation
Barangay officials	Design clarity and applicability	3.5	Agree
Barangay officials	System testing and reliability	3.7	Strongly Agree
Barangay officials	Hardware and software performance	3.6	Strongly Agree
MDRRMO personnel	Output clarity	3.23	Agree
MDRRMO personnel	Usefulness for decision-making	3.49	Agree
MDRRMO personnel	Accuracy and reliability	3.37	Agree

These findings confirm that the system aligns with the barangay-to-MDRRMO reporting workflow. The UAV captures aerial flood images, the ground station processes EXIF-tagged data, the AI module generates flood assessment outputs, and the results can support local disaster response decisions.

4. Conclusion

This study developed and evaluated a UAV-based aerial imaging system integrated with AI-assisted analysis for rapid flood inundation assessment using EXIF-tagged imagery and drone-to-satellite comparison. The system combined UAV image acquisition, geospatial metadata processing, satellite reference comparison, and AI-generated flood interpretation to support the barangay-to-MDRRMO disaster reporting workflow in Pampanga, Philippines.

The results showed that the UAV platform performed reliably across the tested altitudes of 20 m, 40 m, 60 m, 80 m, and 100 m above ground level, achieving a 100% success rate in flight trials. The platform maintained low altitude variability and demonstrated stable hover performance, indicating its suitability for controlled aerial image acquisition during flood observation.

Image quality testing showed that 1920×1080 resolution provided the most suitable image output for AI-assisted flood interpretation, producing the lowest noise value and clearer visual details compared with lower-resolution settings. Ground coverage also increased with flight altitude, from 673.15 m² at 20 m to 17,525.4 m² at 100 m, demonstrating the capability of the UAV to capture wider flood-affected areas at higher altitudes.

The AI-assisted flood analysis showed strong performance in detecting flood and non-flood conditions. All tested AI models achieved 100% flood/non-flood detection accuracy, while GPT 4.1 Nano obtained the fastest mean response time of 7.36 s. For drone-to-satellite comparison, Llama-4-Maverick achieved the highest mean alignment score of 92.2%, followed by GPT 4.1

with 90%, showing that AI-supported satellite comparison can strengthen the spatial validation of UAV-captured flood imagery.

Flood level estimation results showed that most AI models achieved 100% accuracy, while Phi-4-Multimodal-Instruct produced unreliable flood level estimation results. This finding indicates that AI-assisted flood level estimation can support preliminary flood assessment, but model selection and validation remain necessary before operational use in disaster response.

Expert evaluation by barangay officials and MDRRMO personnel showed that the system was generally acceptable for flood monitoring and decision support. Barangay officials rated the system from Agree to Strongly Agree, with overall means ranging from 3.50 to 3.70, while MDRRMO personnel rated the system as Agree, with overall means ranging from 3.23 to 3.49. These results indicate that the developed system is useful, reliable, and applicable within the local flood reporting and assessment workflow.

Overall, the developed UAV-AI system demonstrated its potential as a rapid aerial flood assessment tool for local disaster response. By integrating aerial imaging, EXIF metadata, AI-based interpretation, and drone-to-satellite comparison, the system can provide visual, geospatial, and structured flood assessment outputs that may help improve situational awareness and support faster decision-making during flood events. Future improvements may focus on upgrading the analog video transmission system to digital transmission, improving GPS accuracy and camera calibration, enhancing real-time or offline AI processing, expanding the system into web or mobile platforms, and conducting broader field validation in other flood-prone areas.

5. Acknowledgement

The authors sincerely thank the MDRRMO of Minalin, Pampanga and the Barangay of Paligui, Apalit, Pampanga for their assistance and cooperation during the conduct of this study.

The authors also extend their gratitude to the research adviser, panel members, and faculty evaluators for their guidance, comments, and recommendations that helped improve this research.

References

[1] Schumann, G. J.-P. 2024. Breakthroughs in satellite remote sensing of floods. Frontiers in Remote Sensing. 4: 1280654. DOI: 10.3389/frsen.2023.1280654.

[2] United Nations Office for the Coordination of Humanitarian Affairs. 2025. Philippines: Tropical Cyclones and Floods Revised Humanitarian Needs and Priorities, November 2024–April 2025. United Nations Office for the Coordination of Humanitarian Affairs.

[3] Republic of the Philippines. 2010. Republic Act No. 10121: Philippine Disaster Risk Reduction and Management Act of 2010. Official Gazette/Lawphil.

[4] Wienhold, K. J., D. Li, W. Li, and Z. N. Fang. 2023. Flood Inundation and Depth Mapping Using Unmanned Aerial Vehicles Combined with High-Resolution Multispectral Imagery. Hydrology. 10 (8): 158. DOI: 10.3390/hydrology10080158.

[5] Zhang, Z., and C. Wang. 2024. Research on Flood Disaster Monitoring and Early Warning Technology Based on UAV Remote Sensing and AI Algorithm. International Journal of Communication Networks and Information Security. 16 (2): 19–32.

[6] Camera & Imaging Products Association. 2026. Exchangeable Image File Format for Digital Still Cameras: Exif Version 3.1. CIPA DC-008-Translation-2026. Camera & Imaging Products Association; Esri. 2026. World Imagery. ArcGIS Documentation.

[7] International Organization for Standardization, International Electrotechnical Commission, and Institute of Electrical and Electronics Engineers. 2023. ISO/IEC/IEEE 15288:2023 Systems and Software Engineering—System Life Cycle Processes. Geneva: International Organization for Standardization.

[8] International Council on Systems Engineering. 2023. Systems Engineering Handbook: A Guide for System Life Cycle Processes and Activities. 5th ed. Hoboken, New Jersey: Wiley.

[9] Bjarnason, E., R. Wnuk, and B. Regnell. 2023. Requirements Are Slipping Through the Gaps—A Case Study on Causes and Effects of Communication Gaps in Large-Scale Software Development. Empirical Software Engineering. 28: 1–34.

[10] Republic of the Philippines. 2010. Republic Act No. 10121: Philippine Disaster Risk Reduction and Management Act of 2010. Manila: Republic of the Philippines.

[11] Esri. 2026. World Imagery. ArcGIS Documentation.

[12] Civil Aviation Authority of the Philippines. 2025. CAAP Memorandum Circular No. 026-2025: Remotely Piloted Aircraft System Operations. Manila: Civil Aviation Authority of the Philippines.